Supplementary Information

Competition between dissolution and ion exchange during low temperature synthesis of $LiCoO_2$ on porous carbon scaffolds

Ishita Kamboj, Seongbak Moon, Hannah Denhartog and Veronica Augustyn*

Dept. of Materials Science and Engineering, North Carolina State University, Raleigh, NC USA 27695

* corresponding author e-mail: vaugust@ncsu.edu

Table S1. Quantities of LiOH required to produce a series of solutions (**Figure 3a**) with varying molar ratios of Li^+ to Co^{2+}, molarities, and resulting pH values.

mol ratio of Li^+/Co^{2+}	Mass of LiOH added (mg)	Molarity of LiOH solution (mM)	pH before $Co(OH)_2$ addition	pH on Day 14 (7 days at room temperature, 7 days 60°C)	pH on Day 22 (after an additional 8 days at 60°C)
0	0.00	0	7.25	6.93	8.62
0.002324	0.02	0.001	10.5	8.17	9.06
0.004647	0.05	0.002	10.67	8.48	9.33
0.025	0.45	1.08	11.11	9.71	9.6
0.05	0.90	2.15	11.48	10.41	10.25
0.5	9.03	21.52	12.38	11.7	10.96
1	18.06	43.03	12.43	12.21	11.76
1.5	27.09	64.55	12.44	12.3	12.42
2	36.11	86.07	12.33	12.32	12.58
2.5	45.14	107.56	12.34	12.3	12.54
3	54.17	129.10	12.32	12.3	12.58
3.5	63.20	150.62	12.25	12.28	12.52
4	72.23	172.21	12.22	12.24	12.49
4.5	81.26	193.66	12.18	12.19	12.5
5	90.29	215.17	12.14	12.19	12.44

Estimation of the porous carbon electrochemical surface area from the double layer capacitance

The electrochemical surface area (A) of the porous carbon scaffold was estimated from the double layer capacitance (C_{dl}) of the scaffold obtained in 1 M Na_2SO_4 at 50 mV/s. In most cases, C_{dl} was calculated by taking the integral of the anodic current (*I*) between two voltages (in this example calculation V_1 = 0.2 V, V_2 = 0.4 V) and dividing by the scan rate (*v*) and voltage window (V_2-V_1):

$$C_{dl} = \frac{\int_{V_1}^{V_2} I dV}{v(V_2 - V_1)} \quad (1)$$

The porous carbon electrochemical surface area was then determined by assuming a surface-area normalized capacitance for carbon of 40 μF/cm^2:[1]

$$A = \frac{C_{dl}}{C_s} \quad (2)$$

The mass-normalized electrochemical surface area (A_M) was then obtained by dividing the electrochemical surface area A by the mass of the carbon scaffold (M):

$$A_M = \frac{A}{M} \quad (3)$$

An example of this calculation for CFOAM35 HTC graphite foam is shown below:

$$C_{dl} = \frac{0.001222\ C}{0.2\ V} = 0.006112\ F \quad (4)$$

$$A = \frac{6112\ \mu F}{40 \frac{\mu F}{cm^2}} = 153\ cm^2 = 0.0153\ m^2 \quad (5)$$

$$A_M = \frac{0.0153\ m^2}{0.48353\ g} = 0.0316\ \frac{m^2}{g} \quad (6)$$

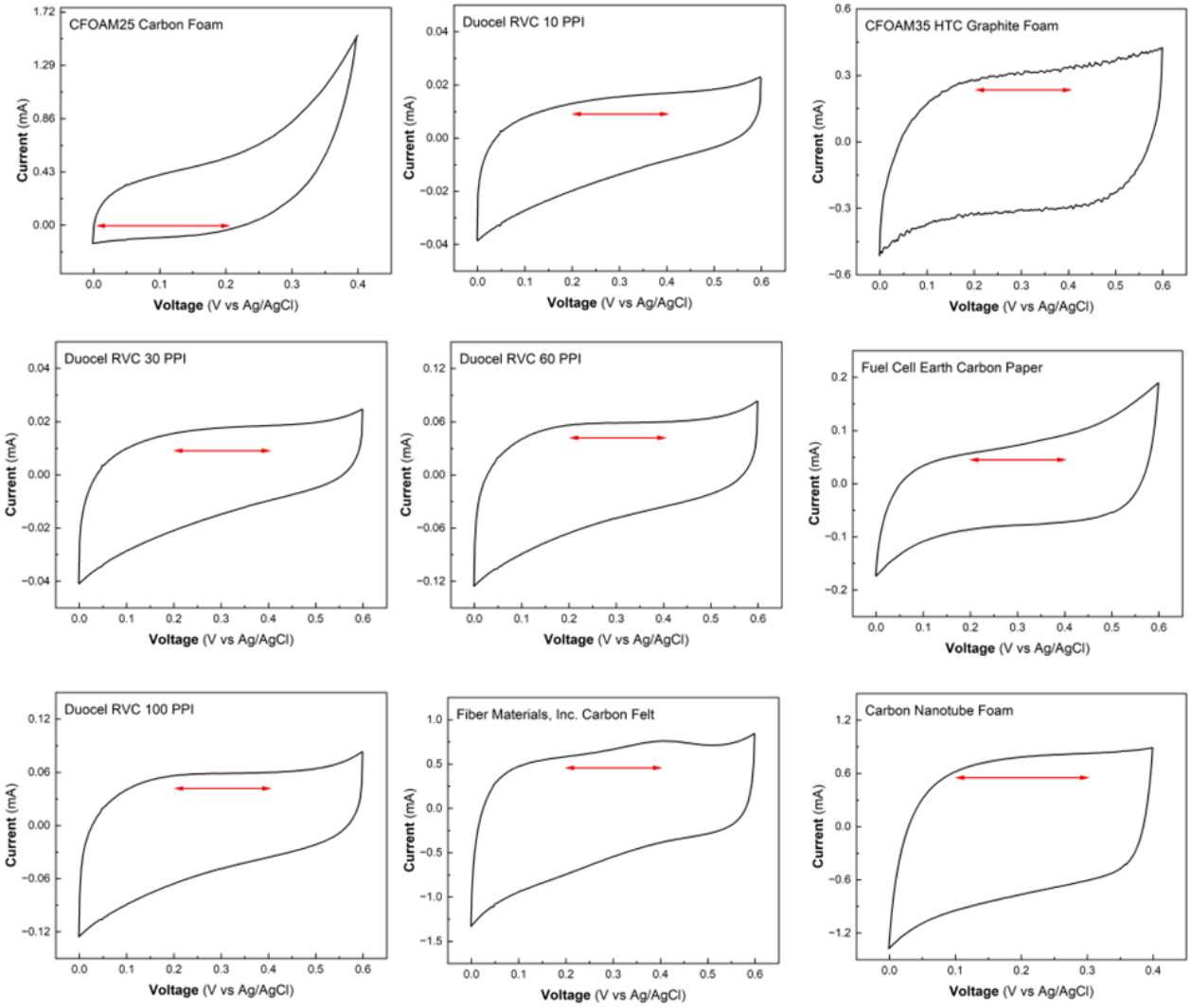

Figure S1. CVs of carbon scaffolds in 1 M Na_2SO_4 at 50 mV/s. The region used for the integration to obtain C_{dl} is shown with red arrows.

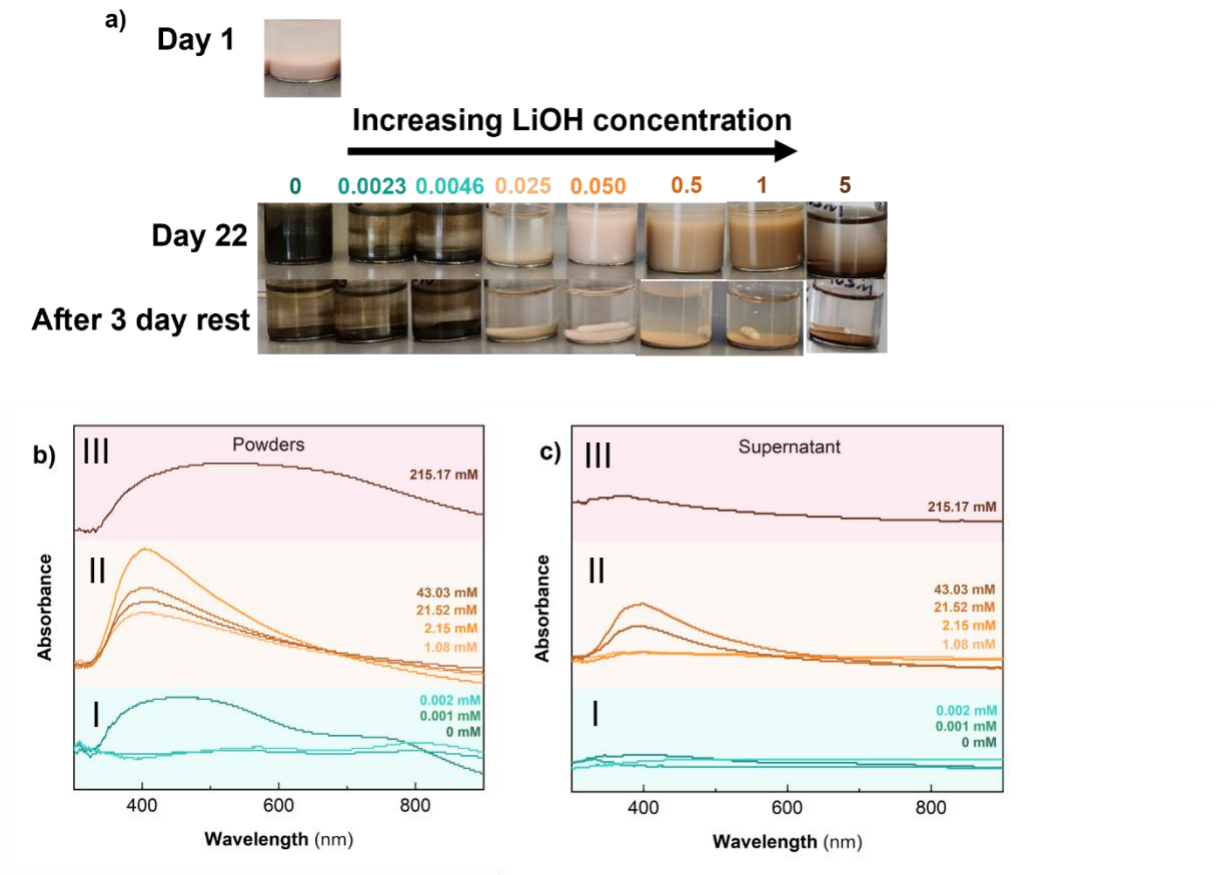

Figure S2. a) Photos of β-$Co(OH)_2$ in LiOH prior to stirring (Day 1), after 22 days of stirring in various LiOH concentrations, and after 3 days of rest following the stirring, where all particles settle to the bottom of vials. There is a color gradient and differences in particle suspension as the LiOH concentration increases. b) UV-Vis spectra of the powders and c) supernatant. The color changes of the powders in a) corresponded to the different proposed reaction mechanisms split into 3 categories in b) and c): conversion of $Co(OH)_2$ to Co_3O_4 (Region 1, green), partial dissolution of $Co(OH)_2$ (Region 2, yellow), and partial oxidation to form CoOOH (Region 3, pink).

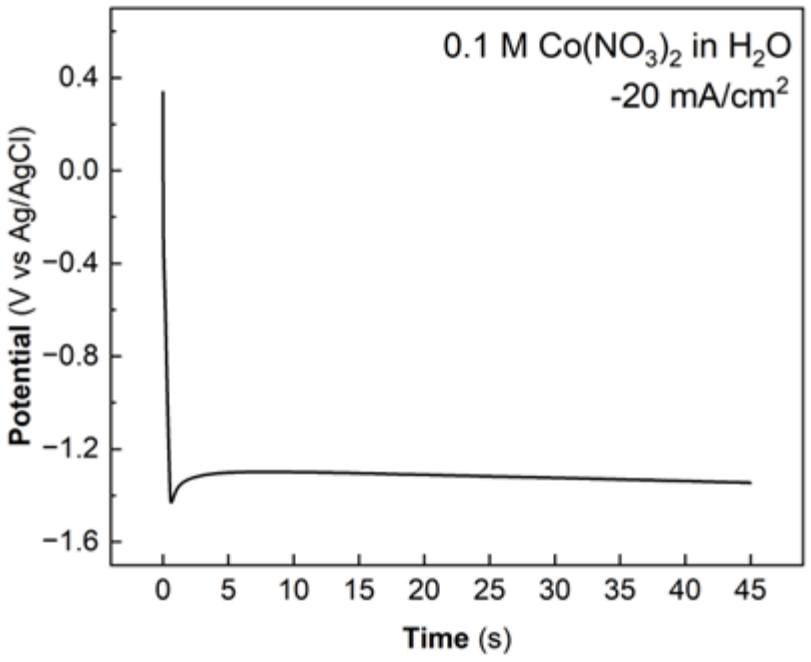

Figure S3. The chronopotentiometric electrodeposition of α-$Co(OH)_2$ from aqueous cobalt nitrate onto carbon paper.

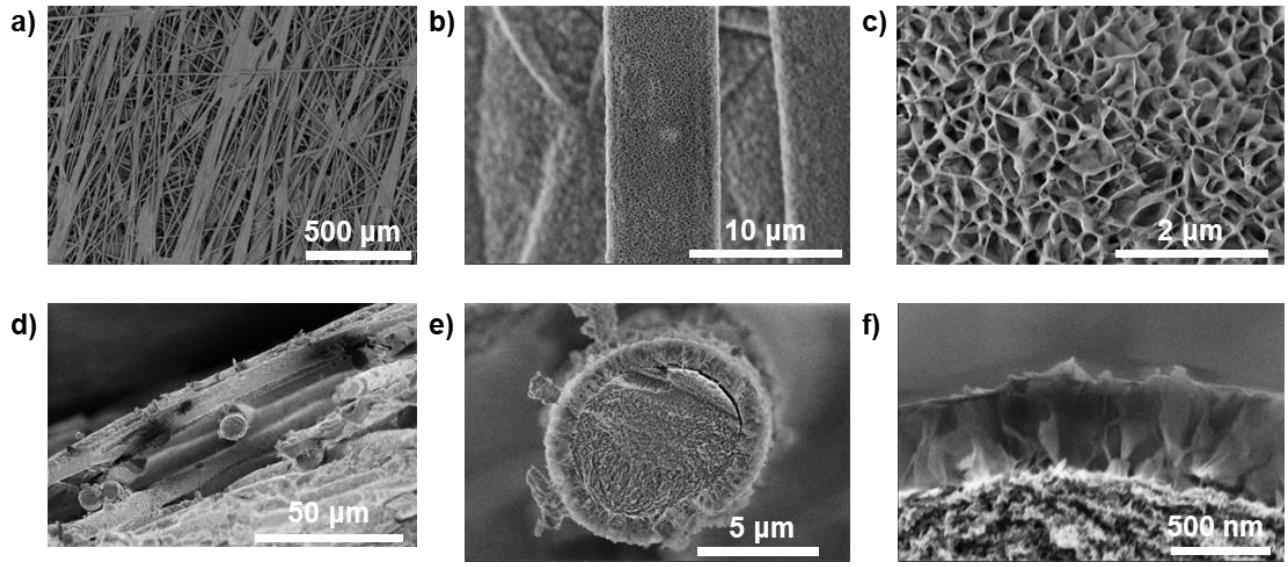

Figure S4. Chronopotentiometric electrodeposition of α-$Co(OH)_2$ from aqueous cobalt nitrate yielded a continuous, conformal coating of nanoflakes onto the carbon paper scaffold. a-c) Top view and d-f) cross-sectional SEM of α-$Co(OH)_2$ nanoflakes on carbon paper after the 45 second electrodeposition shown in **Figure S3**.

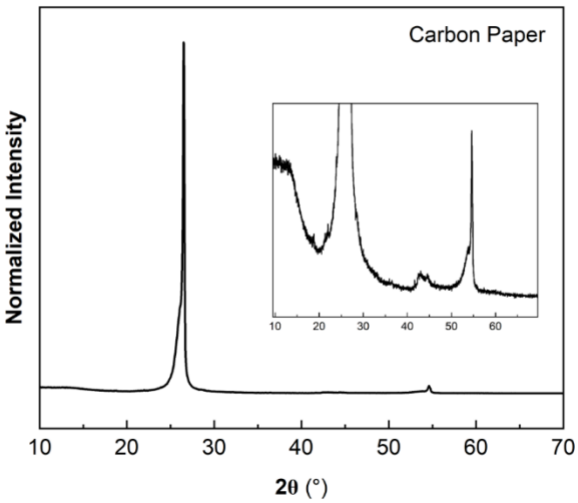

Figure S5. XRD pattern of carbon paper.

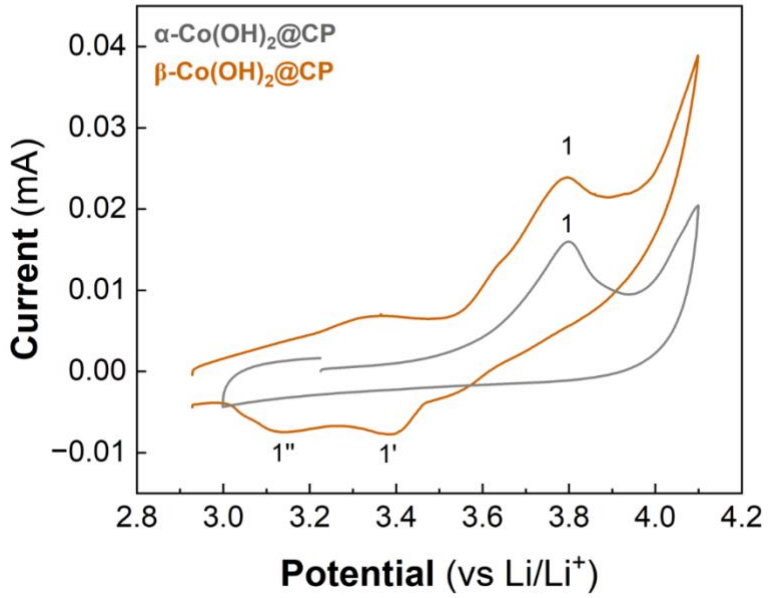

Figure S6. Cyclic voltammograms of an electrode made by soaking electrodeposited α-$Co(OH)_2$@CP (gray curve) and β-$Co(OH)_2$@CP (orange curve) in 4.4 M LiOH under ambient temperature and pressure for 120 h.

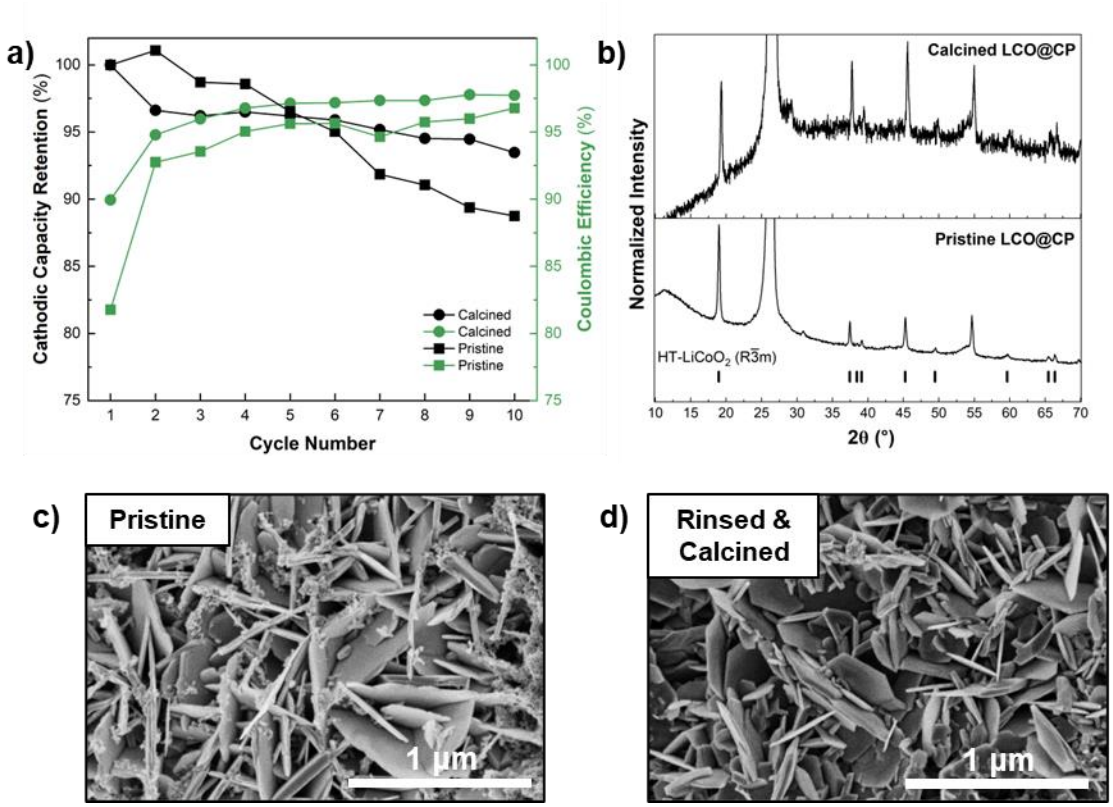

Figure S7. The influence of calcination at 300°C for 8 hours in air on LCO@CP electrodes made by hydrothermal treatment of α-$Co(OH)_2$@CP with 11% fill of 4.4 M LiOH. a) Capacity retention (black) and coulombic efficiency (green) for the pristine (squares) and calcined (circles) electrodes plotted against cycle number show that calcination protocol marginally improves both metrics. b) XRD of pristine (bottom, taken with PANalytical Empyrean) and calcined (top, taken with X'Pert) show crystalline, layered LCO. SEM images show that the nanoflake morphology is present in both the c) pristine and d) rinsed and calcined electrodes. The rinsing procedure described in the Methods is effective at removing excess salt that is present after the hydrothermal treatment.

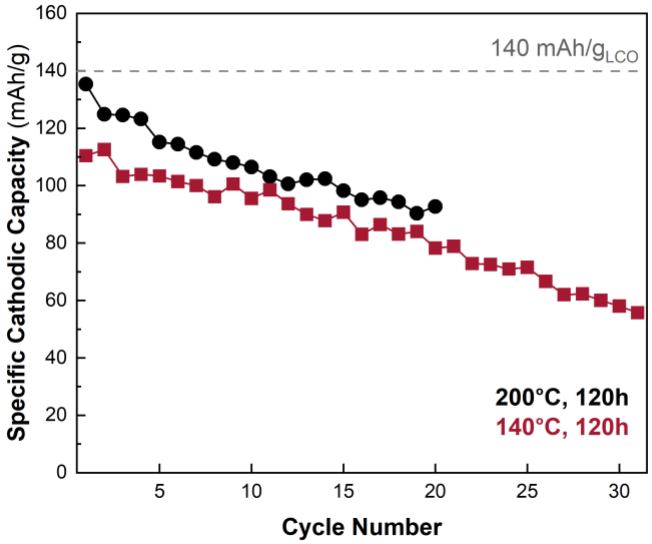

Figure S8. Extended cycling of LCO@CP electrodes made at different hydrothermal synthesis temperatures and duration while pressure and LiOH concentration remained constant (11% vessel fill and 4.4 M LiOH). Cycling was performed using cyclic voltammetry at 0.1 mV/s. All electrodes were tested in a three-electrode configuration with Li metal counter and reference electrodes in 1 M $LiClO_4$ in PC. Capacities were calculated from CVs run at 0.1 mV/s. The dashed horizontal line indicates the practical specific capacity of LCO. The electrode produced at 200˚C for 120 h has better cycling stability over 20 cycles compared to the electrode produced at 140˚C for 120 h.

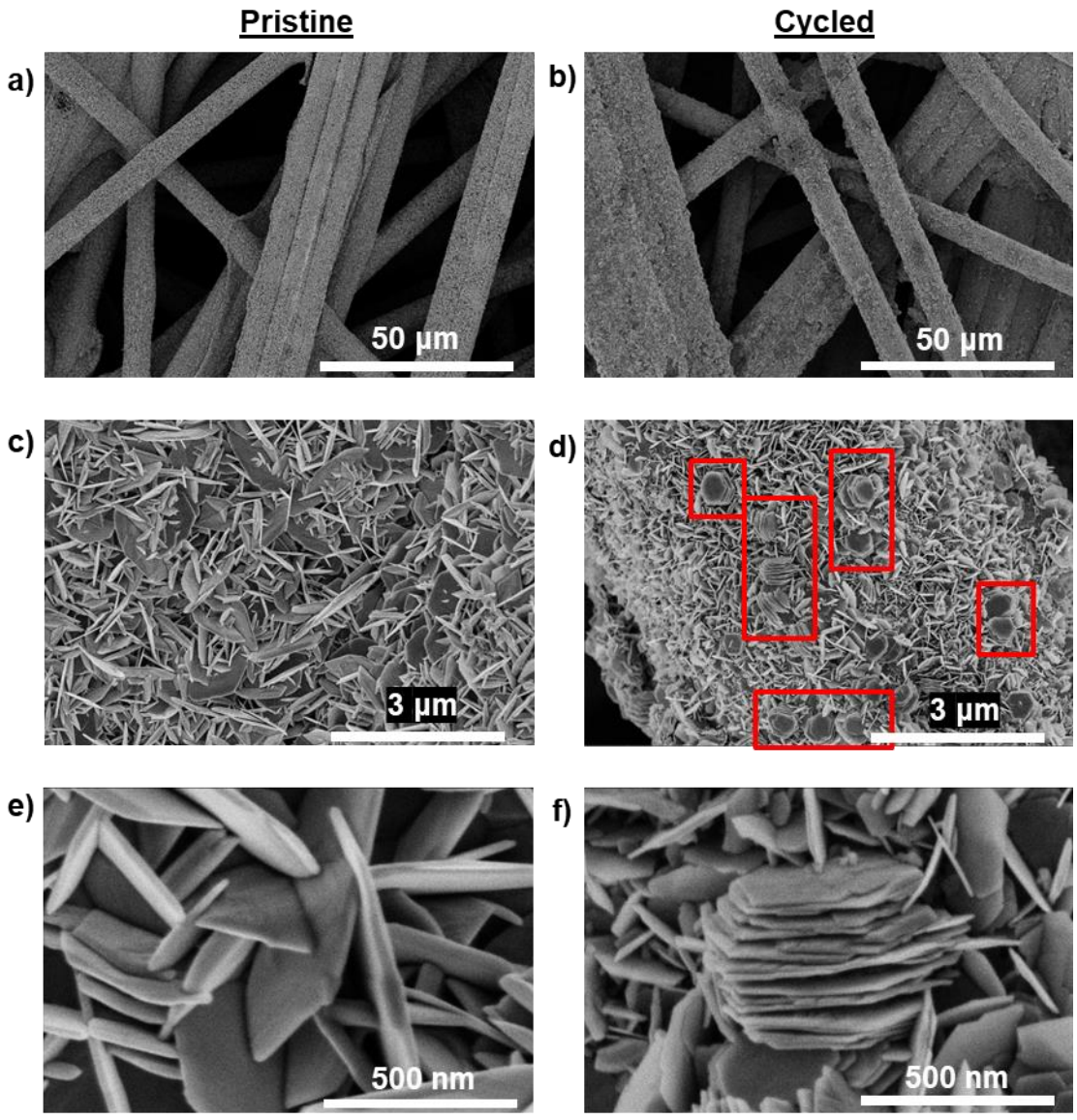

Figure S9. Secondary electron SEM images of a LCO@CP electrode made from hydrothermal synthesis of α-$Co(OH)_2$@CP in 11% fill of 4.4 M LiOH at 200˚C for 15 h: a,c,e) as-synthesized and b,d,f) after ten CV cycles. After cycling, some nanoflakes detached from the matrix and formed agglomerates that decorated the electrode surface.

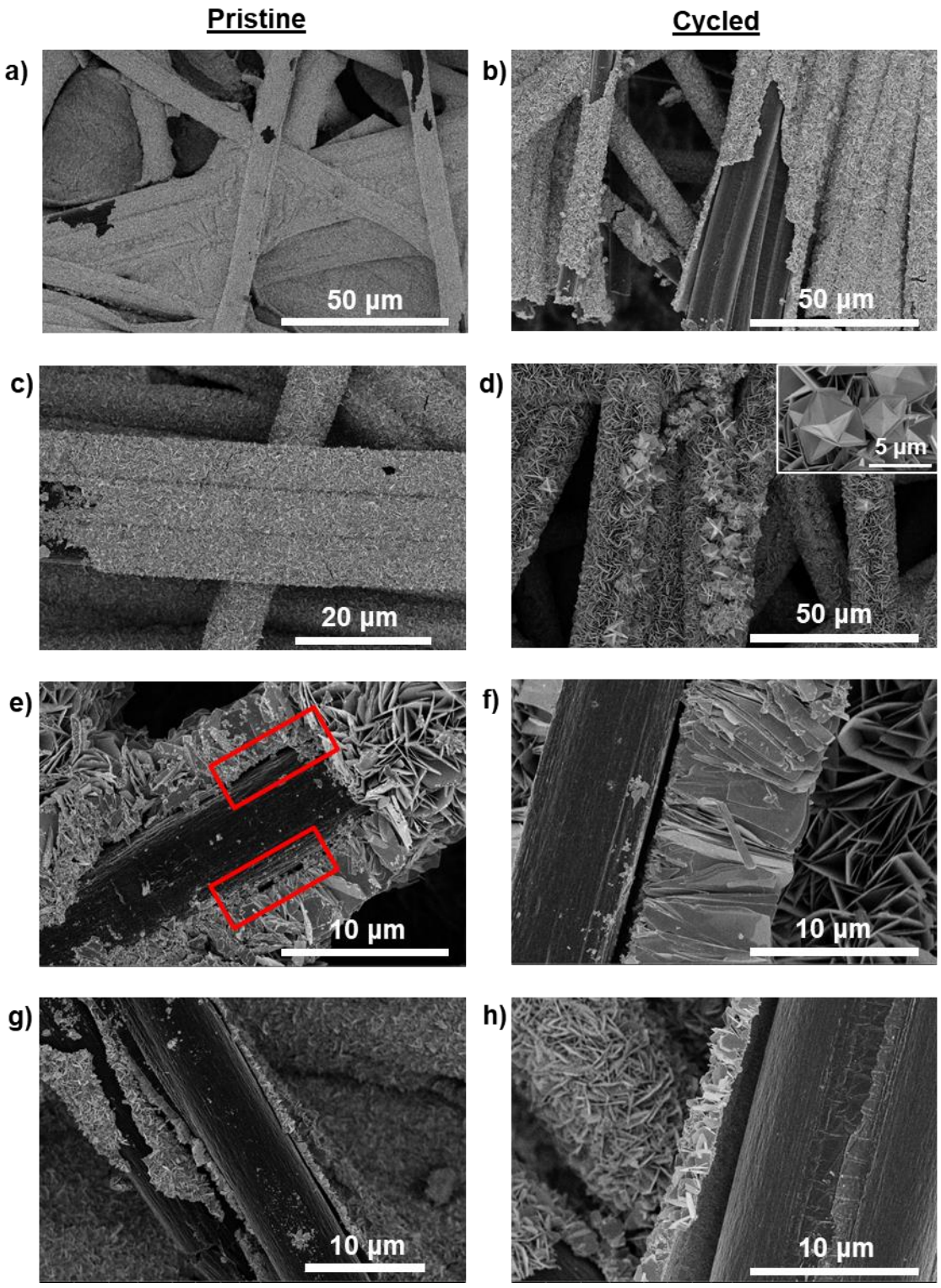

Figure S10. Secondary electron SEM images of of a LCO@CP electrode made from hydrothermal synthesis of α-$Co(OH)_2$@CP in 11% fill of 4.4 M LiOH at 200˚C for 120 h: a,c,e,g) as-synthesized and b,d,f,h) after ten CV cycles. Both pristine and cycled electrodes show

segments where the nanoflake matrix detached entirely from the scaffold. After cycling, some nanoflakes detached from the matrix and formed agglomerates decorating the surface.

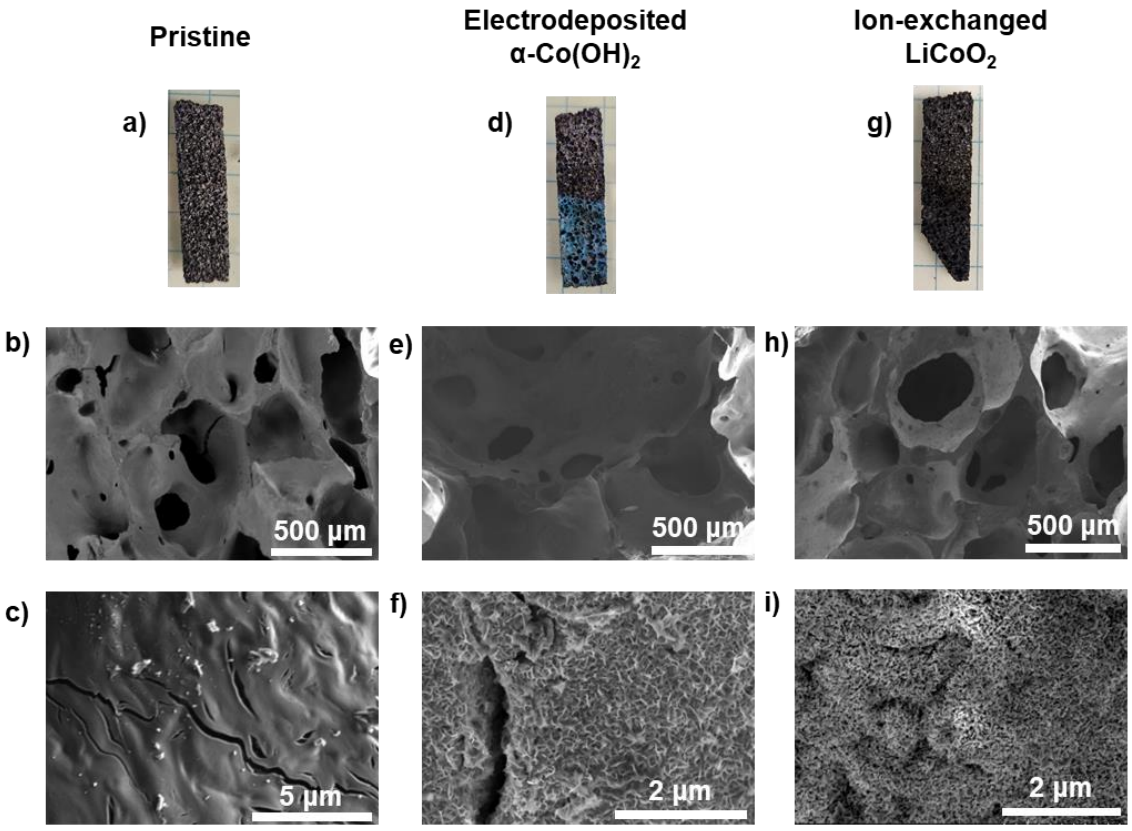

Figure S11. Additional optical (top row) and SEM (middle rows) images taken of a-c) pristine CFOAM25 Carbon Foam scaffold, d-f) after electrodeposition of α-$Co(OH)_2$, and g-i) after hydrothermal treatment for 15 hours at 200˚C in 4.4 M LiOH in H_2O (11% reactor fill) to produce ion-exchanged LCO.. The first row of SEM are backscattered electron images to better highlight depth in the scaffold, and the second row are secondary electron images.

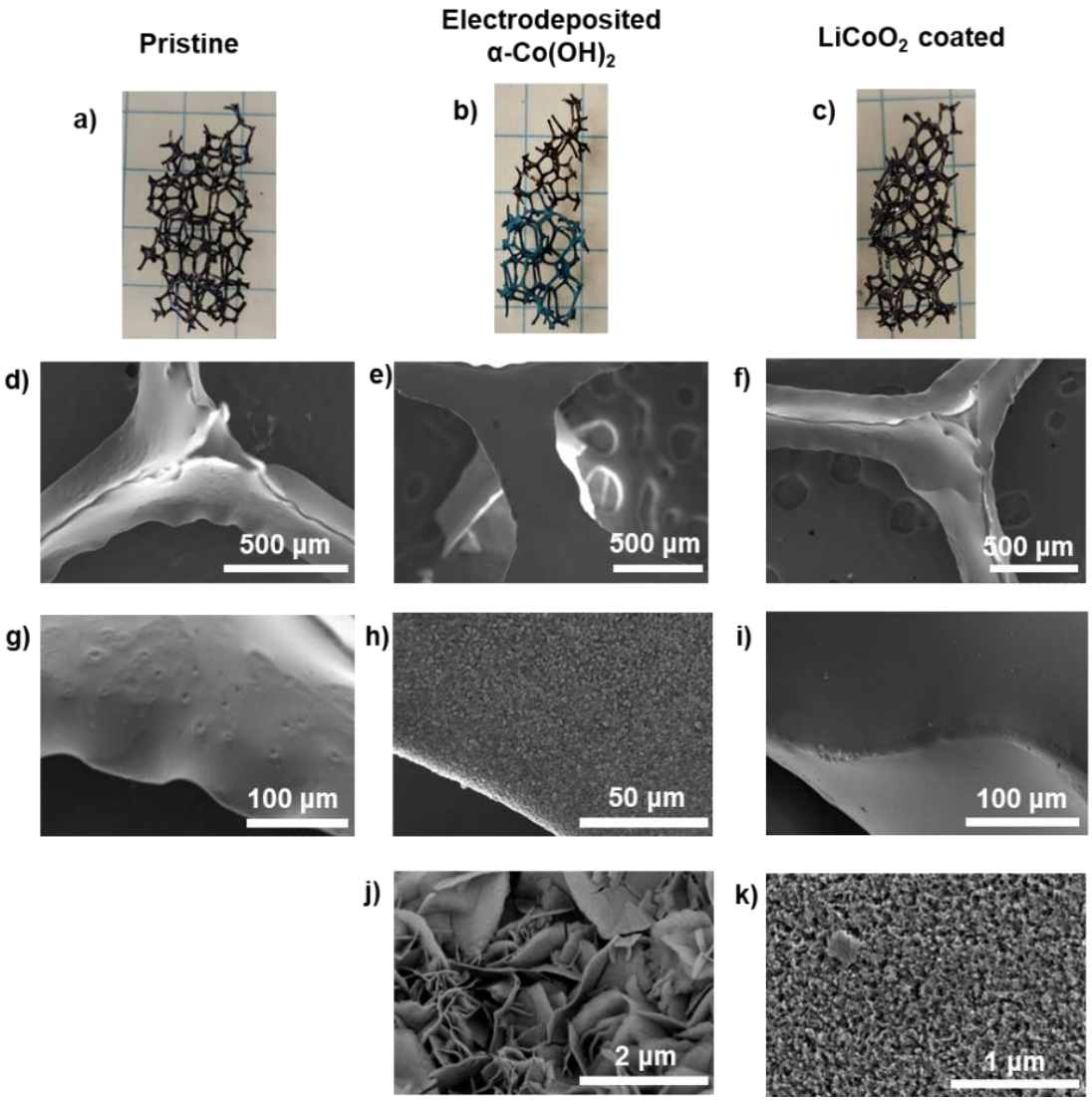

Figure S12. Additional optical (top row) and SEM (other rows) images taken of a,d,g) pristine Duocel RVC 10 PPI scaffold, b,e,h,j) after electrodeposition of α-$Co(OH)_2$, and c,f,i,k) after hydrothermal treatment for 15 hours at 200˚C in 4.4 M LiOH in H_2O (11% reactor fill) to produce LCO. All SEM images are backscattered electron images except k, which is a secondary electron image to better highlight the morphology of the LCO formed.

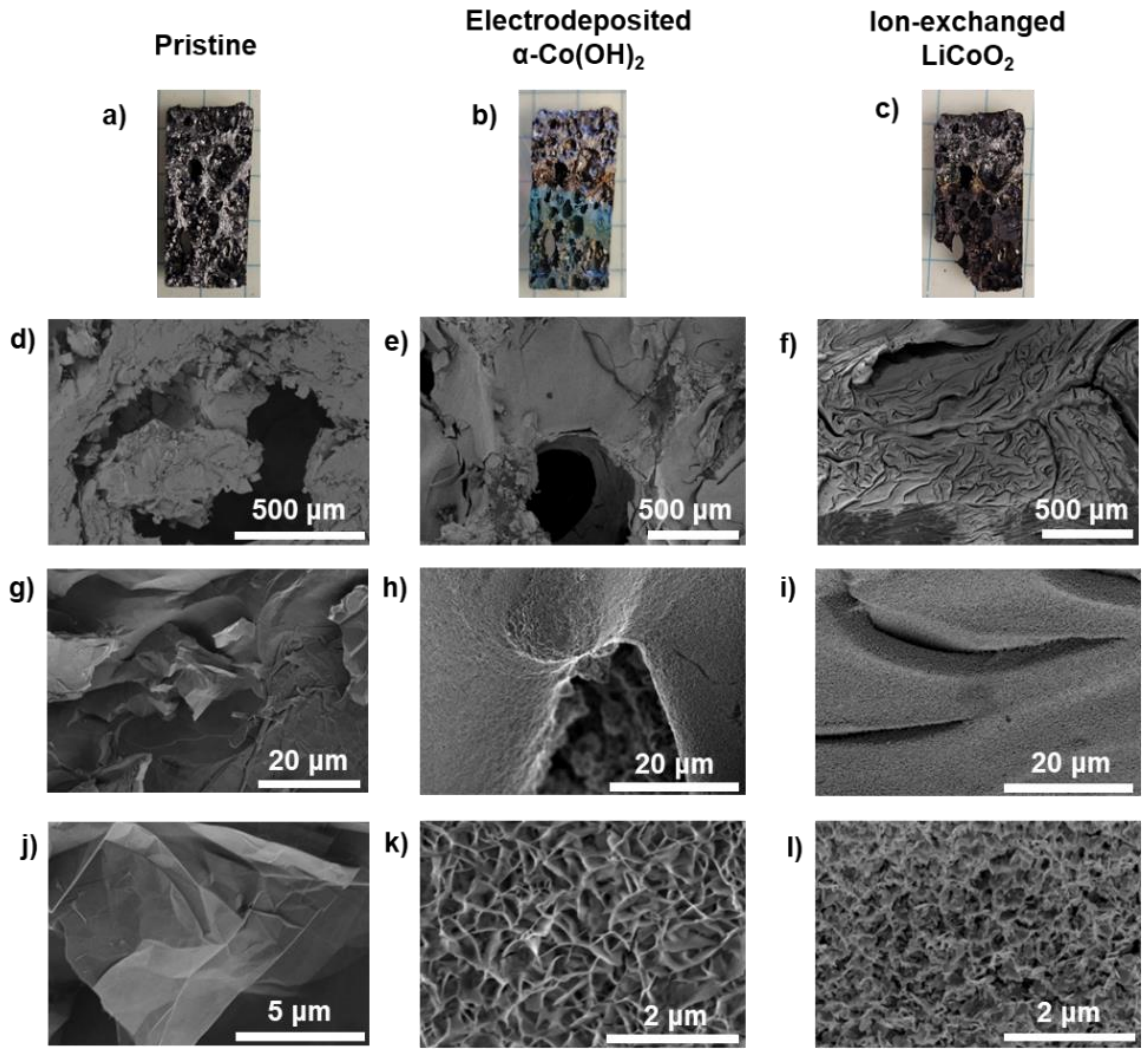

Figure S13. Additional optical (top row) and SEM (middle rows) images taken of a,d,g,j) pristine CFOAM35 HTC Graphite Foam scaffold, b,e,h,k) after electrodeposition of α-$Co(OH)_2$, and e,f,i,l) after hydrothermal treatment for 15 hours at 200˚C in 4.4 M LiOH in H_2O (11% reactor fill) to produce ion-exchanged LCO. The first row of SEM are backscattered electron images to better highlight depth in the scaffold, and the other two rows are secondary electron images.

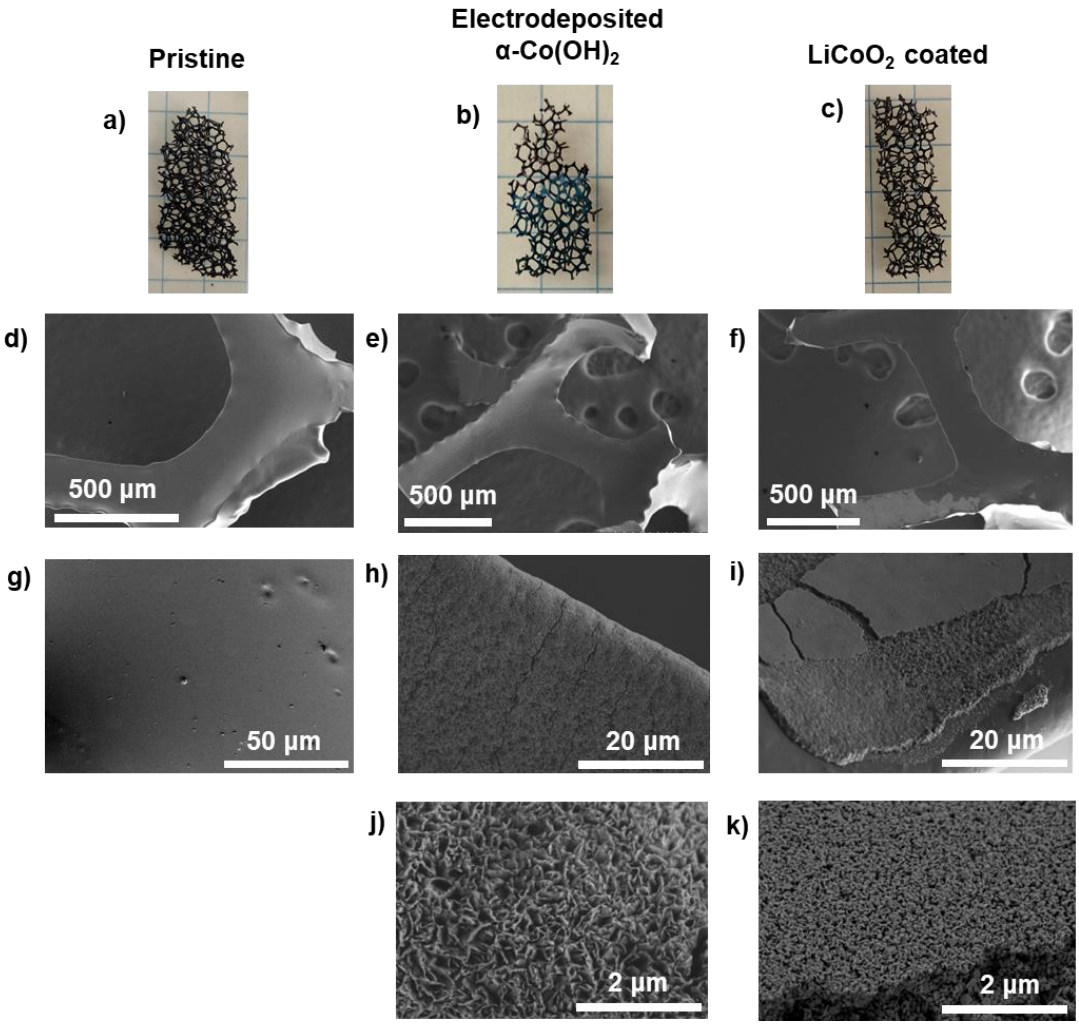

Figure S14. Additional optical (top row) and SEM (other rows) images of a,d,g) pristine Duocel RVC 30 PPI scaffold, b,e,h,j) after electrodeposition of α-$Co(OH)_2$, and c,f,i,k) after hydrothermal treatment for 15 hours at 200˚C in 4.4 M LiOH in H_2O (11% reactor fill) to produce LCO.

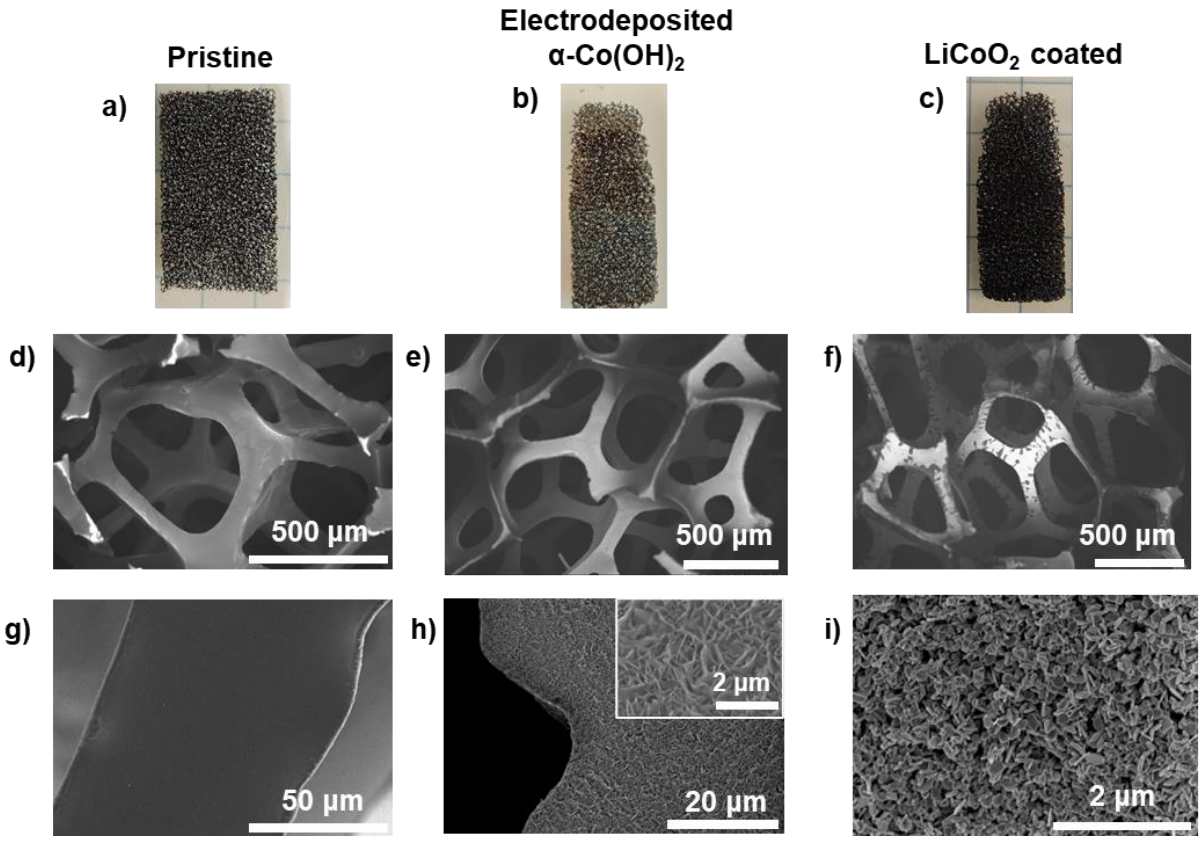

Figure S15. Additional optical (top row) and SEM (middle rows) images of a,d,g) pristine Duocel RVC 60 PPI scaffold, b,e,h) after electrodeposition of α-$Co(OH)_2$, and c,f,i) after hydrothermal treatment for 15 hours at 200˚C in 4.4 M LiOH in H_2O (11% reactor fill) to produce LCO. All SEM images shown are secondary electron images.

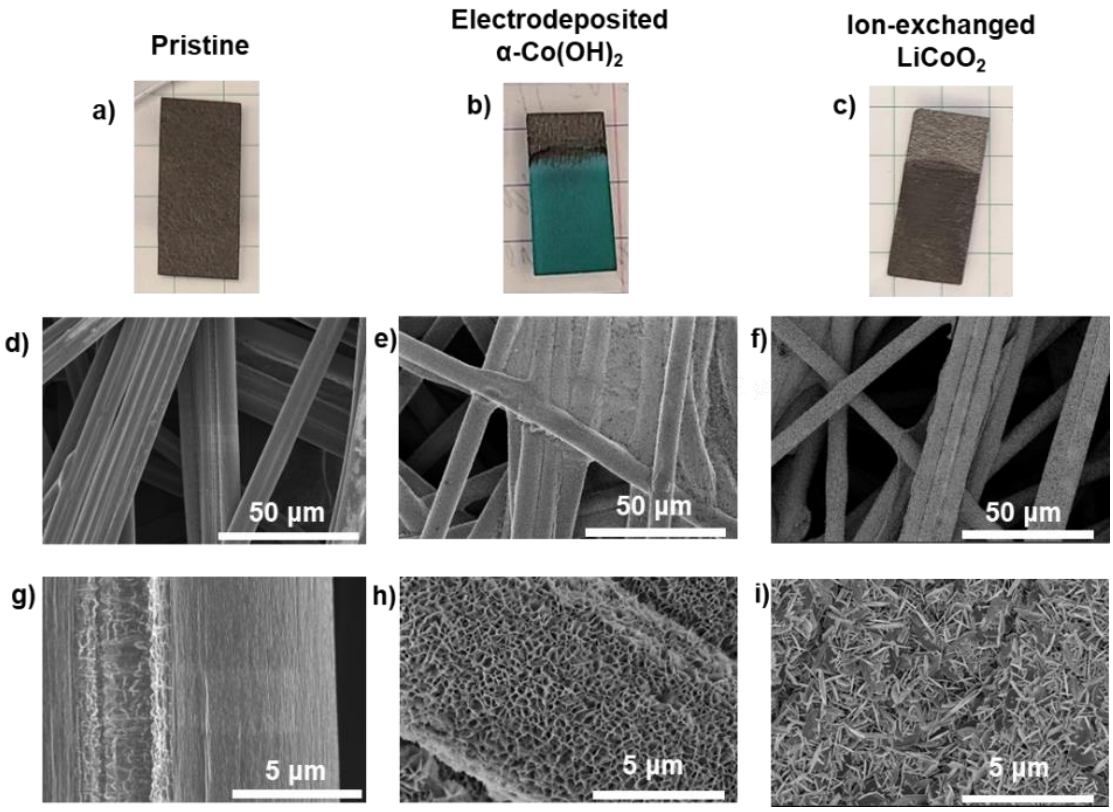

Figure S16. Additional optical (top row) and SEM (middle rows) images of a,d,g) pristine Fuel Cell Earth AvCarb MGL190 carbon paper scaffold, b,e,h) after electrodeposition of α-$Co(OH)_2$, and c,f,i) after hydrothermal treatment for 15 hours at 200˚C in 4.4 M LiOH in H_2O (11% reactor fill) to produce ion-exchanged LCO. All SEM images shown are secondary electron images.

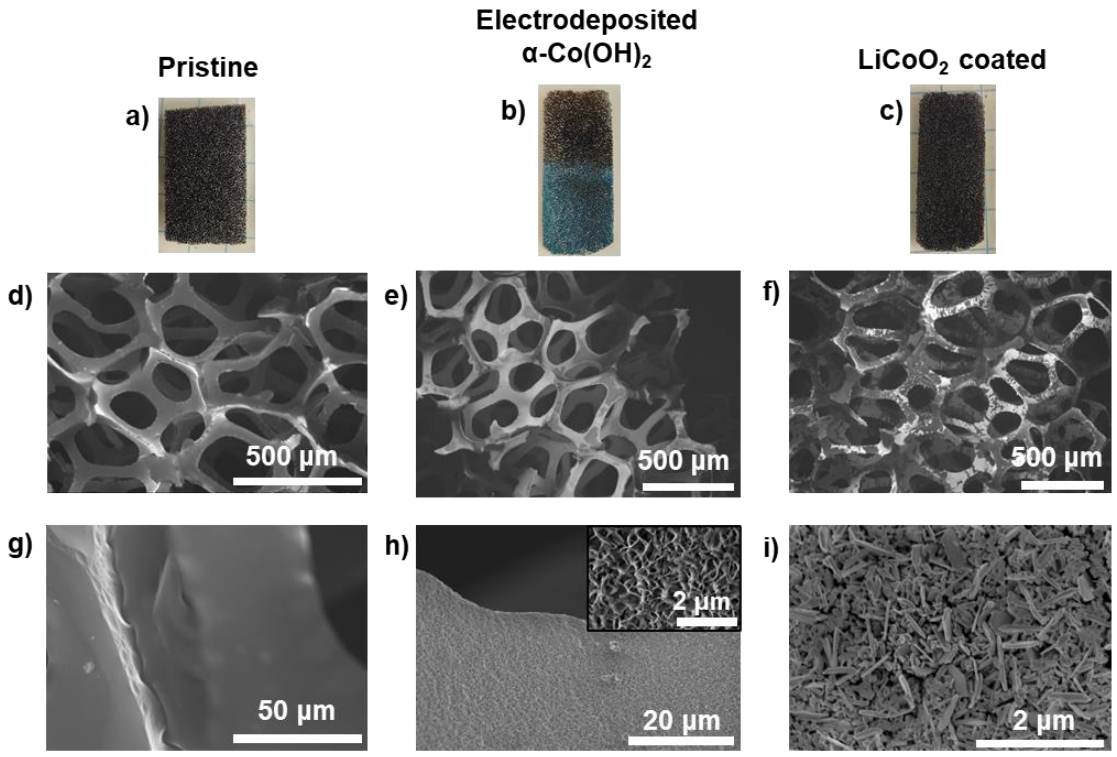

Figure S17. Additional optical (top row) and SEM (middle rows) images of a,d,g) pristine Duocel RVC 100 PPI scaffold, b,e,h) after electrodeposition of α-$Co(OH)_2$, and c,f,i) after hydrothermal treatment for 15 hours at 200˚C in 4.4 M LiOH in H_2O (11% reactor fill) to produce LCO. All SEM images shown are secondary electron images.

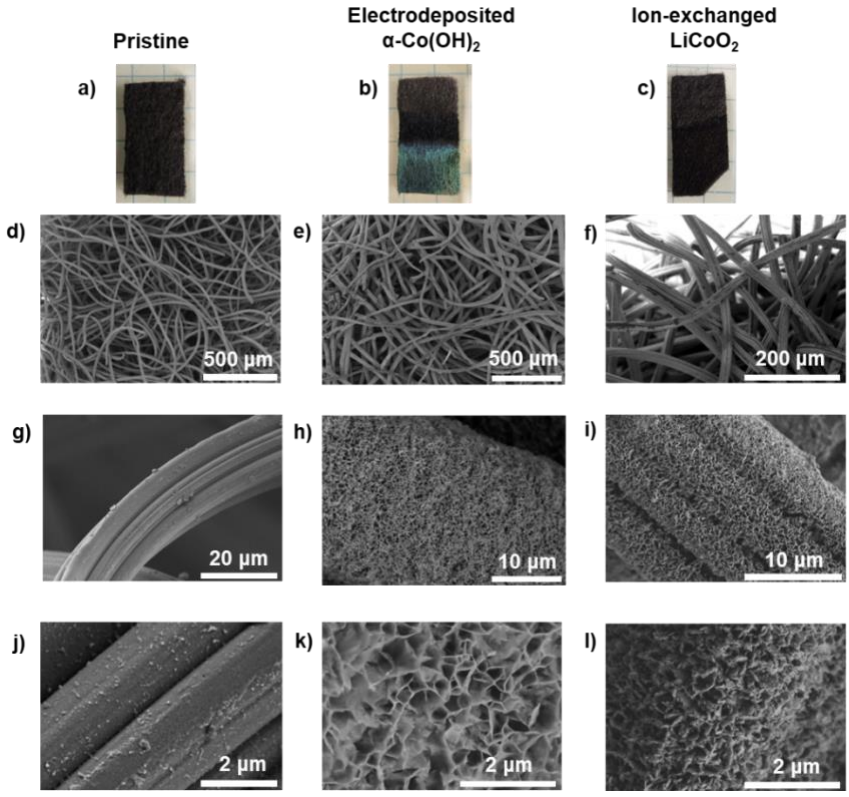

Figure S18. Additional optical (top row) and SEM (middle rows) images of a,d,g,j) pristine carbon felt scaffold, b,e,h,k) after electrodeposition of α-$Co(OH)_2$, and c,f,i,l) after hydrothermal treatment for 15 hours at 200˚C in 4.4 M LiOH in H_2O (11% reactor fill) to produce ion-exchanged LCO. The first row of SEM images shown are backscattered electron images to better illustrate depth of the scaffold, and the rest are secondary electron images.

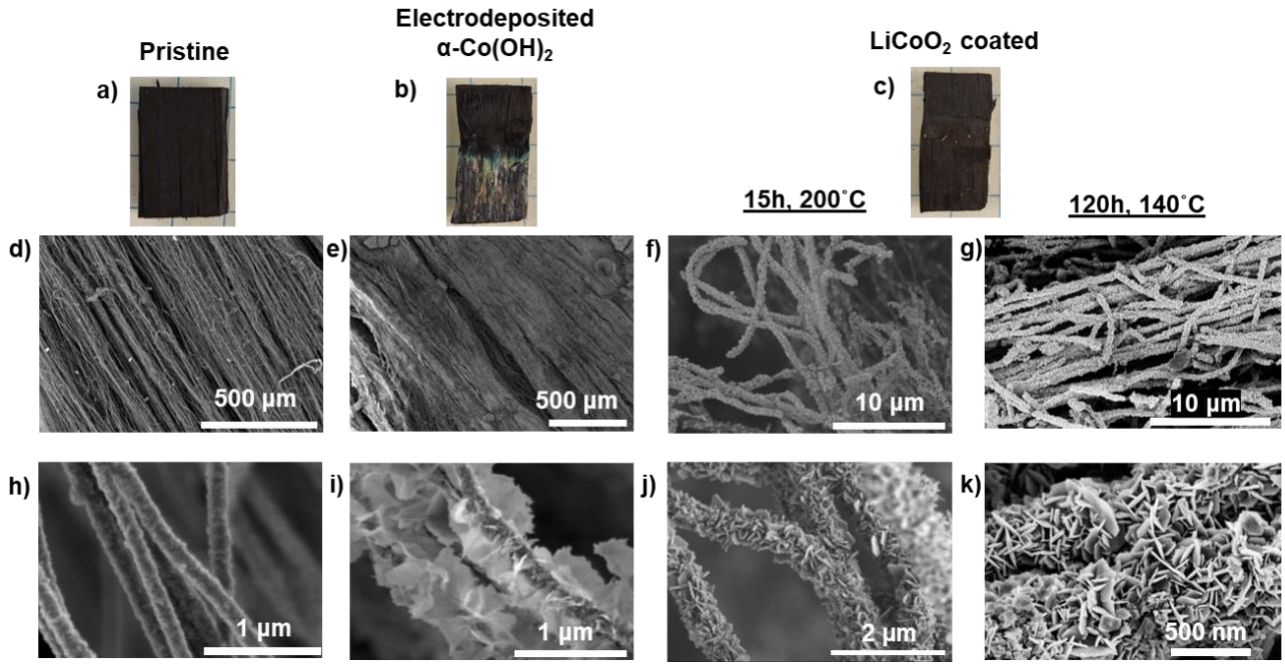

Figure S19. Additional optical (top row) and SEM (middle rows) images of a,d,h) pristine carbon nanotube foam scaffold, b,e,i) after electrodeposition of α-$Co(OH)_2$ and c,f,j) after hydrothermal treatment for 15 hours at 200˚C in 4.4 M LiOH in H_2O (11% reactor fill) to produce ion-exchanged LCO. g,k) Additional SEM images of ion-exchanged $LiCoO_2$ produced via hydrothermal treatment of electrodeposited α-$Co(OH)_2$ on a carbon nanotube foam scaffold for 120 hours at 140˚C in 4.4 M LiOH in H_2O (11% reactor fill).

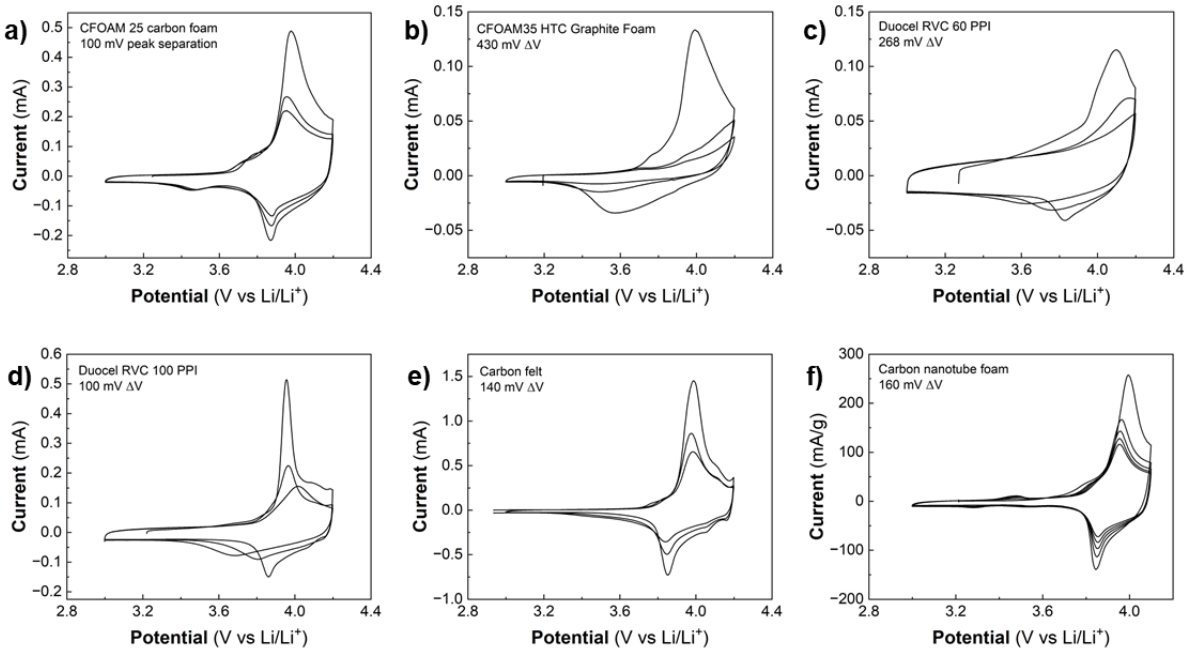

Figure S20. Cyclic voltammograms of LCO on various carbon scaffolds. a-e) CVs of 3 cycles at 0.1 mV/s in 1 M $LiClO_4$ in PC. Electrodes were synthesized by hydrothermal treatment of electrodeposited α-$Co(OH)_2$ for 15 hours at 200˚C in 4.4 M LiOH in H_2O (11% reactor fill). f) CV of 5 cycles under the same conditions as a-e after hydrothermal treatment of electrodeposited α-$Co(OH)_2$ on a carbon nanotube foam scaffold for 120 hours at 140˚C in 4.4 M LiOH in H_2O (11% reactor fill). All electrodes exhibit a redox couple around 3.9 V in the first cycle indicating the formation of HT-LCO except b) CFOAM35 HTC Graphite Foam.

Supplementary Information Reference

1. B. E. Conway, Electrochemical Supercapacitors, Springer US, Boston, MA, 1999.